Hologram recording with mutually orthogonal polarized waves in $Sr_{0.61}Ba_{0.39}Nb_2O_6$:Ce

F. Kahmann, J. Höhne, R. Pankrath, and R. A. Rupp
Fachbereich Physik der Universität Osnabrück, 49069 Osnabrück, Federal Republic of Germany
(Received 6 April 1994)

$Sr_{0.61}Ba_{0.39}Nb_2O_6$:Ce exhibits pronounced dichroism which is strongly correlated with the cerium concentration. This property triggers effective hologram recording with mutually orthogonal polarized writing beams via self-diffraction. We measure the saturation diffraction efficiency, using an extraordinarily polarized readout beam, versus the polarization of the recording beams. The experimental results are compared to straightforward theoretical models based on linear dichroism including self-diffraction. We show that the saturation diffraction efficiency is strongly enhanced by self-diffraction effects.

Photorefraction in electro-optic materials is intensively investigated in order to exploit this effect for future applications on the one hand and to improve the understanding of the underlying mechanisms on the other. If holographic methods are used for material characterization and investigation, usually two coherent light beams interfere within the sample forming a spatially varying intensity distribution. This in turn leads to redistribution of photocarriers due to drift, diffusion, and the photovoltaic effect. Finally, a space-charge field is left behind which causes a refractive index grating via the electro-optic effect.

Contrarily, if two mutually orthogonal polarized writing beams intersect inside a sample, no spatial intensity modulation appears, but the information is encoded within a spatial variation of the polarization state of the total light field.[1] Such a polarization hologram has been utilized to record refractive index gratings via nondiagonal components of the photovoltaic tensor in Fe-doped $LiNbO_3$ (Ref. 2) and $KNbO_3$.[3] The writing beams in this geometry are polarized in parallel with and perpendicular to the c-axis, respectively.

In this contribution, we report on a recording mechanism using mutually orthogonal polarized writing beams in $Sr_{0.61}Ba_{0.39}Nb_2O_6$:Ce. We attribute the recording process to self-diffraction effects induced by linear dichroism.

Utilizing a CARY-17D spectrometer we measured the optical absorption for ordinarily (Fig. 1) and extraordinarily polarized incoherent light waves for a set of $Sr_{0.61}Ba_{0.39}Nb_2O_6$:Ce samples grown with different CeO_2 content in the melt (Table I). All samples have been produced in the crystal laboratory of the University of Osnabrück using the Czochralski method. The absorption in the range of 400–700 nm increases linearly with the CeO_2 concentration in the melt, which means that the distribution coefficient is constant up to 0.2 wt % CeO_2 in the melt. We notice a pronounced difference between the absorption spectra for ordinarily and extraordinarily polarized light as depicted in Fig. 2. This linear dichroism is strongly correlated with the CeO_2 content in the melt, too.

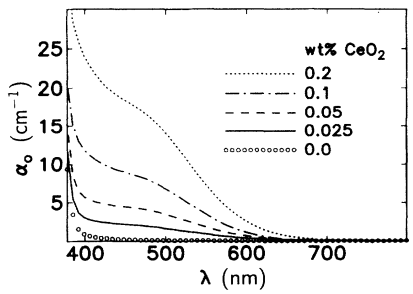

FIG. 1. Absorption spectra for $Sr_{0.61}Ba_{0.39}Nb_2O_6$:Ce samples grown from melts with different CeO_2 contents (Table I) using ordinarily polarized incoherent light.

In order to record elementary holograms we use a common two-beam interference setup as sketched in Fig. 3. The writing beams R and S of equal intensities and of wavelength $\lambda_w = 515$ nm have mutually orthogonal polarization. The c-axis of the sample is parallel to the grating vector $\mathbf{K}$ and within the plane of incidence.

An elementary hologram of grating spacing $\Lambda = 2\pi/|\mathbf{K}| = 1.8\ \mu$m is recorded. A third beam of wavelength $\lambda_r = 633$ nm, not shown in Fig. 3 for simplicity, reads out the previously recorded hologram. This readout beam is extraordinarily polarized taking advantage of the linear electro-optic coefficient r_{33} to obtain maximal diffraction efficiency (Table II). The diffraction efficiency is defined as

$$\eta = \frac{I_S}{I_S + I_R}\ , \tag{1}$$

where I_S and I_R are the diffracted and transmitted intensities behind the sample. Successive recording and read-

TABLE I. Doping and size of the samples used.

Sample	Doping wt % CeO_2 in the melt	Size $a \times b \times c$/mm^3
SBN 5.1	0.00	5.5×5.7×7.2
SBN 12.1	0.025	3.0×5.5×4.3
SBN 13.1	0.05	2.4×4.4×4.1
SBN 15.1	0.1	2.8×5.3×4.9
SBN 16.2	0.2	1.5×5.3×4.1

TABLE II. Linear electro-optic coefficients (in Voigt's notation) as measured with a Mach-Zehnder interferometer.

Sample	r_{13}/pm V^{-1} at λ 515 nm	633 nm	r_{33}/pm V^{-1} at λ 515 nm	633 nm
SBN 15.1	55±5		260±20	240±20

ing cycles are performed for different settings of φ_R, which is the angle between the polarization orientation of beam R and the normal of the plane of incidence (Fig. 3). The measured saturation diffraction efficiency η as a function of φ_R is represented by full dots in Fig. 4. Independently of φ_R the Bragg-diffracted beam remains always extraordinarily polarized, i.e., there is only isotropic diffraction.

As the writing beams are not polarized in parallel with the crystal axis, both beams inside the crystal split up into their eigenmodes of ordinary and extraordinary polarization. Ordinarily and extraordinarily polarized components interfere by pairs, each forming an intensity variation with spatial frequency $K=|\mathbf{K}|$ but with a relative phase mismatch of π (Fig. 5):

$$\begin{aligned} I_o(z,x)&=I_o(x)[1+m_o(x)\cos Kz]\,,\\ I_e(z,x)&=I_e(x)[1-m_e(x)\cos Kz]\,,\\ I_p(x)&=I_{p,R}(x)+I_{p,S}(x)\,,\\ m_p(x)&=2\sqrt{I_{p,R}(x)I_{p,S}(x)}/I_p(x)\,, \end{aligned} \tag{2}$$

with $p=(e,o)$. The total intensity distribution is the sum of both intensity variations

$$\begin{aligned} I(z,x)&=I_o(z,x)+I_e(z,x)=I(x)[1+m(x)\cos Kz]\,,\\ I(x)&=I_o(x)+I_e(x)\,, \end{aligned} \tag{3}$$

$$m(x)=\frac{I_o(x)m_o(x)-I_e(x)m_e(x)}{I(x)} =2\frac{\sqrt{I_{o,R}(x)I_{o,S}(x)}-\sqrt{I_{e,R}(x)I_{e,S}(x)}}{I_{o,R}(x)+I_{o,S}(x)+I_{e,R}(x)+I_{e,S}(x)}\,.$$

Though the total modulation degree may in general range from $+1$ to -1, note that initially, i.e., at $x=0$, there is no modulation at all, i.e., we have $m(0)=0$.

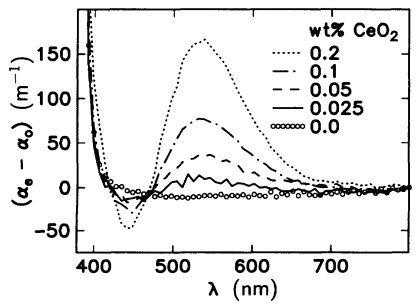

FIG. 2. Difference between the absorption coefficients of extraordinarily and ordinarily polarized incoherent light $\alpha_e-\alpha_o$ versus wavelength. $Sr_{0.61}Ba_{0.39}Nb_2O_6$:Ce samples grown with different CeO_2 content in the melt (Table I) are used.

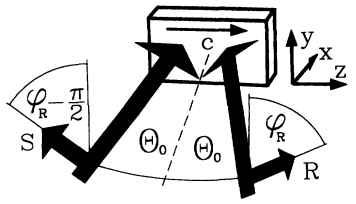

FIG. 3. Sketch of the recording arrangement. Waves R and S are mutually orthogonal polarized.

The spatially modulated intensity $\Delta I(x)=m(x)I(x)$ generates a spatially modulated electrical current $\Delta j(x)=\Delta\sigma(x)E_{SC}(x)$ via diffusion as the dominant transport mechanism of photocarriers in $Sr_xBa_{1-x}Nb_2O_6$:Ce,[4] where $\Delta\sigma(x)$ is the first Fourier component of the photoconductivity. The space-charge field

$$E_{SC}(x)=-m(x)Kk_BT/e \tag{4}$$

induces a refractive index change

$$\Delta n(x)=-(1/2)n^3r_{33}E_{SC}(x) \tag{5}$$

via the linear electro-optic effect, where k_B, T, e, and n are Boltzmann's constant, temperature, electron charge, and refractive index, respectively.

For an isotropic medium the generation of the grating depends only on the intensity amplitude ΔI. This does not necessarily hold for anisotropic media, since the photoconductivity may depend on the polarization state of the incident light. However, we observed no significant difference in the specific photoconductivity between ordinarily and extraordinarily polarized light for the sample used (Table III). The photoconductivity was measured by applying an external electric field to the sample. We monitored the steady-state photocurrent during illumination of the sample.

Our geometry of mutually orthogonal polarized writing beams of equal intensities leads to an unmodulated total intensity in front of the sample, $m(0)=0$, as it is expected for mutually orthogonal polarized waves (Fig. 5).

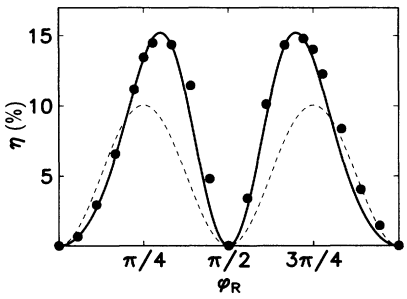

FIG. 4. Dots represent experimental values of the saturation diffraction efficiency as a function of φ_R (Fig. 3) for elementary holograms recorded with mutually orthogonal polarized waves in SBN 15.1 (Table I). The broken line is a theoretical curve that considers the effect of linear dichroism and holographic scattering, only. The full line results from a model which additionally takes self-diffraction into account.

TABLE III. Specific photoconductivities in SBN 15.1 for ordinarily and extraordinarily polarized light.

Sample	$(\sigma_o^{ph}/I)/10^{-11}$ m V^{-2} at λ: 440 nm	515 nm	$(\sigma_e^{ph}/I)/10^{-11}$m V^{-2} at λ: 440 nm	515 nm
SBN 15.1	1.9±0.3	0.98±0.2	2.05±0.3	0.96±0.2

However, the attenuation for ordinarily and extraordinarily polarized light as a function of thickness differs because of the linear dichroism. This means that in general

$$I_e(x)=I_e(0)\exp(-\alpha_e x/\cos\Theta_e) \neq I_o(x)=I_o(0)\exp(-\alpha_o x/\cos\Theta_o) .$$

Here Θ_e and Θ_o are the angles of incidence of extraordinarily and ordinarily polarized waves within the sample, respectively. As we have $I_e(0)=I_o(0)$, the modulation degree does not vanish within the sample, i.e., $m(x>0)\neq 0$ (Fig. 5).

Additionally, strong light scattering is observed in $Sr_{0.61}Ba_{0.39}Nb_2O_6$:Ce as shown in Fig. 6. Furthermore, the scattering phenomenon is anisotropic in the sense that it predominantly appears for extraordinarily polarized light. In Fig. 6, the transmission of the SBN 15.1 sample is measured for incidence of an ordinarily and extraordinarily polarized laser beam, respectively, as a function of time. We measure pronounced depletion in intensity behind the sample for extraordinarily polarized light. In order to take this effect into account we introduce an additional extinction coefficient $\tilde{\alpha}_e$ which describes the exponential attenuation as a function of thickness for extraordinarily polarized light in the case of saturation: $I_e(x)=I_e(0)\exp(-\tilde{\alpha}_e x/\cos\Theta_e)$ with $\tilde{\alpha}_e=\alpha_e+\alpha_{e,\text{scatt}}$. From Fig. 6 we determine $\alpha_{e,\text{scatt}}=170$ m^{-1}, while scattering is nearly absent for ordinarily polarized light and we put $\tilde{\alpha}_o=\alpha_o$.

A recorded grating is characterized by measuring the diffraction efficiency η, which is given by Kogelnik's formula[5]

$$\eta=\sin^2(\nu),\quad \nu=\frac{\pi\Delta n d}{\lambda_r\cos\Theta_e} . \tag{6}$$

This formula has been deduced with a constant refractive index modulation Δn as a function of thickness. This does not hold in our case since the refractive index change $\Delta n(x)$ [Eqs. (4) and (5)], which is proportional to the modulation degree $m(x)$ [Eq. (3)], depends on the thickness of the sample.

In the following, we restrict our considerations to the approximation of small angles of incidence: $\cos\Theta_p\approx 1$, with $p=(e,o)$. Based on the theory of coupled waves,[5] beam propagation through the sample is given by a set of differential equations for the complex field amplitudes (omitting the argument of the complex field amplitudes for simplicity)

$$\begin{bmatrix} dR_p/dx \\ dS_p/dx \end{bmatrix} = \begin{bmatrix} -\tilde{\alpha}_p/2 & -i\kappa_p(x)\exp(i\phi) \\ -i\kappa_p(x)\exp(-i\phi) & -\tilde{\alpha}_p/2 \end{bmatrix} \begin{bmatrix} R_p \\ S_p \end{bmatrix} . \tag{7}$$

The derivation of the complex field amplitude of each wave is composed of a transmitted and a Bragg-diffracted contribution. The phase shift between the refractive index grating and the recording interference pattern is denoted by ϕ. In $Sr_xBa_{1-x}Nb_2O_6$:Ce we obtain $\phi=\pi/2$ as diffusion is the main transport mechanism. The coupling coefficients are defined as

$$\kappa_p(x)=\frac{\pi\Delta n_p^{\max}}{\lambda}m(x) . \tag{8}$$

The maximum material response at the wavelength λ for extraordinarily and ordinarily polarized light, respective-

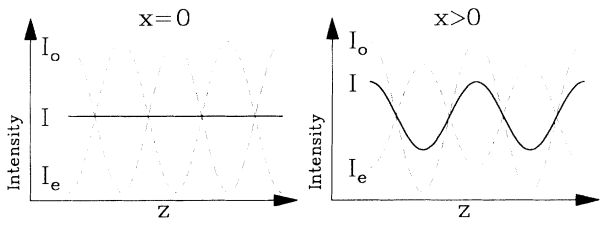

FIG. 5. Ordinarily and extraordinarily polarized components, I_o and I_e, of the total intensity I interfere by pairs. I_o, I_e, and I are shown at $x=0$ mm and $x>0$ mm as a function of z, which is the coordinate parallel to the grating vector.

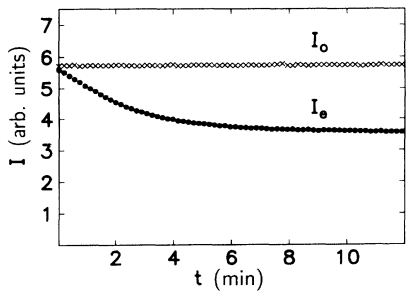

FIG. 6. The intensity is monitored versus time when a single laser beam illuminates the $Sr_{0.61}Ba_{0.39}Nb_2O_6$:Ce sample (SBN 15.1) starting at $t=0$. This experiment is done with ordinarily and extraordinarily polarized light.

ly, is expressed by the magnitude of the maximal refractive index change $\Delta n_p^{\max}$, which is calculated using Eqs. (4) and (5) for the maximal modulation degree of $m=1$. We point out that in our case the coupling coefficients κ_p are functions of the thickness x since they are proportional to the modulation degree $m(x)$.

A change to new variables [$A=(R,S)$]

$$\hat{A}_p(x)=A_p(x)\exp(x\tilde{\alpha}_p/2) \tag{9}$$

simplifies Eq. (7)

$$\begin{bmatrix} d\hat{R}_p/dx \\ d\hat{S}_p/dx \end{bmatrix} = -i\kappa_p(x)M \begin{bmatrix} \hat{R}_p \\ \hat{S}_p \end{bmatrix},$$
$$M=\begin{bmatrix} 0 & \exp(i\phi) \\ \exp(-i\phi) & 0 \end{bmatrix}. \tag{10}$$

The formal solution of Eq. (10) is

$$\begin{bmatrix} \hat{R}_p(x) \\ \hat{S}_p(x) \end{bmatrix} = \begin{bmatrix} \hat{R}_p(0) \\ \hat{S}_p(0) \end{bmatrix} \exp\left[-iM\int_0^x \kappa(x')dx'\right]. \tag{11}$$

With $\hat{S}(0)=0$ and $\hat{R}(0)=1$ we calculate the diffraction efficiency from Eq. (1)

$$\eta=\sin^2(\bar{v}),\quad \bar{v}=\frac{\pi\overline{\Delta n}d}{\lambda_r\cos\Theta_e},$$
$$\overline{\Delta n}=\frac{1}{d}\int_0^d \Delta n(x')dx' \propto \bar{m}. \tag{12}$$

If we compare Eq. (12) to Eq. (6) we notice that Kogelnik's theory still holds. As a result, we take into account a profile in the refractive index amplitude (or the modulation degree) if we insert

$$\bar{m}=\frac{1}{d}\int_0^d m(x)dx, \tag{13}$$

which is the average modulation degree, via Eqs. (4) and (5) in Kogelnik's formula, Eq. (6), to obtain the diffraction efficiency. A more general theory is given by Serdyuk.[6]

In our geometry we have

$$\begin{aligned} I_{o,R}(x)&=I(0)\exp(-\tilde{\alpha}_o x)\cos^2\varphi_R, \\ I_{e,R}(x)&=I(0)\exp(-\tilde{\alpha}_e x)\sin^2\varphi_R, \\ I_{o,S}(x)&=I(0)\exp(-\tilde{\alpha}_o x)\sin^2\varphi_R, \\ I_{e,S}(x)&=I(0)\exp(-\tilde{\alpha}_e x)\cos^2\varphi_R. \end{aligned} \tag{14}$$

The average modulation degree results in

$$\begin{aligned} \bar{m}&=\sin(2\varphi_R)\left[1+\frac{2}{\Delta\alpha d}\ln\left[\frac{1+\exp(-\Delta\alpha d)}{2}\right]\right] \\ &\approx \sin(2\varphi_R)\bar{m}_{\max} \end{aligned} \tag{15}$$

with $\Delta\alpha=\tilde{\alpha}_e-\tilde{\alpha}_o$. It becomes maximal at $\varphi_R=0.25\pi$ and 0.75π with $\bar{m}_{\max}=0.17$ in our experiment. The expected diffraction efficiency is obtained using Eqs. (4)–(6) and is plotted in Fig. 4 as a broken line. Linear electro-optic coefficients for SBN 15.1 (Table I) at $\lambda_r=633$ nm and $\lambda_w=515$ nm are determined by applying an external electrical field parallel to the c-axis and measuring the optical path difference for extraordinarily polarized light in a Mach-Zehnder interferometer (Table II).[7] The results are in good agreement with Refs. 7 and 8.

Obviously, the measured saturation diffraction efficiency η versus φ_R (Fig. 4) mainly exhibits two characteristics that differ from the theoretical curve based on Eq. (15): First, the measured maximum value of the saturation diffraction efficiency $\eta_{\max}$ exceeds the theoretical one. Second, the measured saturation diffraction efficiency as a function of φ_R does not follow $\eta=\sin^2[c\sin(2\varphi_R)]$, which is theoretically expected from Eq. (15), where c is constant. The theory predicts the maximal saturation diffraction efficiency $\eta_{\max}$ at $\varphi_R=0.25\pi$ and 0.75π, whereas the experiment shows $\eta_{\max}$ at $\varphi_R\approx 0.3\pi$ and 0.7π.

In general, the recording process is dynamical: Both writing beams R and S interfere in the medium, generate a refractive index grating, and are in the same time diffracted from that grating. The diffracted fraction of beam R interferes with the transmitted one of beam S (and vice versa) since they are collinear and coherent. Generally, this self-diffraction effect[9,10] leads to a perturbation in intensity and phase of both writing beams as they propagate through the medium. This in turn affects the successive grating recording process within the medium.

The self-diffraction phenomenon is omnipresent, but may be neglected in some cases, especially if the complex field amplitude of a diffracted beam is small compared to that of a transmitted one. This approximation does not hold in our case due to large linear electro-optic coefficients (Table II).

The coupled wave Eqs. (7) for ordinarily and extraordinarily polarized waves do not decouple in pairs since the total modulation degree and hence the coupling coefficients are functions of all complex field amplitudes according to Eqs. (3) and (8). Consequently, ordinarily and extraordinarily polarized waves are coupled by the previously recorded grating. We seek for a self-consistent solution of the coupled wave Eqs. (7) in the steady-state regime.

We separate the complex field amplitudes A_p ($A=R,S$, $p=e,o$) into phase $\psi_{p,A}$ and intensity $I_{p,A}$ with the definition

$$A_p(x)=\sqrt{I_{p,A}(x)}\exp(i\psi_{p,A}). \tag{16}$$

From Eqs. (7) we receive the phase perturbation of the recording beams[10] as $d\psi_{p,A}/dx\propto\cos\phi=0$ due to $\phi=\pi/2$. Changing to new variables

$$\hat{I}_{p,A}(x)=I_{p,A}(x)\exp(\tilde{\alpha}_p x) \tag{17}$$

simplifies Eqs. (7) (arguments of $\hat{I}_{p,A}$ are omitted for simplicity):

$$\begin{aligned} d\hat{I}_{o,R}/dx&=-d\hat{I}_{o,S}/dx=+\Gamma_o(x)\sqrt{\hat{I}_{o,R}\hat{I}_{o,S}}, \\ d\hat{I}_{e,R}/dx&=-d\hat{I}_{e,S}/dx=-\Gamma_e(x)\sqrt{\hat{I}_{e,R}\hat{I}_{e,S}}, \end{aligned} \tag{18}$$

with

$$\Gamma_{e,o}(x)=\frac{2\pi\sin\phi}{\lambda_w}\Delta n_{e,o}^{\max} m(x)\ ,$$
$$m(x)=2\frac{\sqrt{\hat{I}_{o,R}\hat{I}_{o,S}}-\sqrt{\hat{I}_{e,R}\hat{I}_{e,S}}\exp(-\Delta\alpha x)}{\hat{I}_{o,R}+\hat{I}_{o,S}+(\hat{I}_{e,R}+\hat{I}_{e,S})\exp(-\Delta\alpha x)}\ . \tag{19}$$

From Eq. (18) we obtain $d\hat{I}_p/dx=0$ with $\hat{I}_p=\hat{I}_{p,R}+\hat{I}_{p,S}$ which expresses the conservation of energy. Note that conservation of energy for $\hat{I}_p$ holds because the constant absorption coefficient for ordinarily and extraordinarily polarized light, respectively, has been already taken into consideration by the definition of $\hat{I}_p$ in Eq. (17).

The Runge-Kutta method is used for integrating Eqs. (18) and (19) numerically, starting with $\hat{I}_{o,R}(0)=\hat{I}_{e,S}(0)=I(0)\cos^2\varphi_R$ and $\hat{I}_{o,S}(0)=\hat{I}_{e,R}(0)=I(0)\sin^2\varphi_R$. Figure 7 shows the steady-state intensity distribution as a function of the thickness x and the coordinate z parallel to the grating vector **K**. In our case we have maximal intensity coupling ($\sin\phi=1$) but no fringe bending ($\cos\phi=0$). Therefore, we obtain the saturation diffraction efficiency η for the readout beam with the help of Kogelnik's formula Eq. (6) if we use the average modulation degree Eq. (13) to calculate the effective space-charge field from Eq. (4). The average modulation degree $\bar{m}$ is determined from the numerical solution of Eqs. (18) and (19). $\bar{m}$ becomes maximal at $\varphi_R\approx 0.3\pi$ and 0.7π with $\bar{m}_{\max}\approx 0.21$. The expected saturation diffraction efficiency η is plotted as a function of φ_R in Fig. 4 as a full line. This theoretical curve is in good agreement with the experimental values.

The presence of linear dichroism, $\Delta\alpha\neq 0$, initially leads to a nonvanishing modulation degree of the total intensity. This triggers energy exchange between both recording beams via the linear electro-optic effect. The energy exchange may be amplified via self-diffraction since both beams will dynamically adjust in such a way that Eqs. (18) and (19) are fulfilled in the steady-state regime. In our case, two effects contribute to the recording of holograms with mutually orthogonal polarized writing beams: First, linear dichroism and, second, self-diffraction of the recording beams. Hologram formation due to self-diffraction depends on the difference of the corresponding electro-optic coefficients. Consequently, energy exchange and hence hologram creation with mutually orthogonal polarized waves is very effective in the case of large electro-optic coefficients. In this case, only a small dichroitic effect, which is omnipresent, is needed to potentially start hologram buildup via self-diffraction. Enhancement of the recorded hologram due to self-diffraction is observed for properly chosen polarization vectors of the incident beams (like $\varphi_R=0.3\pi$ in our geometry).

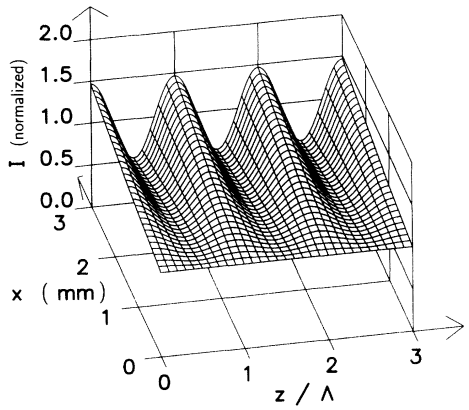

FIG. 7. Theoretically expected steady-state intensity distribution $I(z,x)$ as a function of thickness x and of z, which is the coordinate parallel to the grating vector **K**. The input intensity is normalized to unity. $I(z,x)$ is plotted for $\varphi_R=0.3\pi$ which coincides with the theoretical and experimental maximum of $\eta(\varphi_R)$ (Fig. 4).

As a conclusion, we obtain effective hologram creation with mutually orthogonal polarized beams. The self-diffraction effect, initiated by linear dichroism, is the main mechanism of hologram buildup.

This work has been supported by the Deutsche Forschungsgemeinschaft, SFB 225 (Project A6).

[1]T. Huang and K. Wagner, SPIE **1559**, 377 (1991).
[2]S. G. Odulov, Pis'ma Zh. Eksp. Teor. Fiz. **1**, 10 (1982) [JETP Lett. **35**, 10 (1982)].
[3]U. van Olfen, H. Hesse, G. Jäkel, E. Krätzig, and S. Odoulov, Opt. Commun. **93**, 219 (1992).
[4]M. D. Ewbank, R. R. Neurgaonkar, W. K. Cory, and J. Feinberg, J. Appl. Phys. **62**, 374 (1987).
[5]H. Kogelnik, Bell Syst. Tech. J. **48**, 2909 (1969).
[6]V. M. Serdyuk, Zh. Tekh. Fiz. **59**, 11 (1989) [Sov. Phys. Tech. Phys. **34**, 1097 (1989)].
[7]S. Ducharme, J. Feinberg, and R. R. Neurgaonkar, IEEE J. Quantum Electron. **QE-23**, 2116 (1987).
[8]G. L. Wood, W. W. Clark, M. J. Miller, E. J. Sharp, G. J. Salamo, and R. R. Neurgaonkar, IEEE J. Quantum Electron. **QE-23**, 2126 (1987).
[9]V. L. Vinetskii, N. V. Kukhtarev, S. G. Odulov, and M. S. Soskin, Usp. Fiz. Nauk **129**, 113 (1979) [Sov. Phys. Usp. **22**, 742 (1979)].
[10]P. Günter and J.-P. Huignard, *Photorefractive Materials and Their Applications II*, Topics in Applied Physics Vol. 62 (Springer-Verlag, Berlin, 1989).